

IMECE2009-12765

DESIGN, ANALYSIS AND OPTIMIZATION OF MAGNETIC MICROACTUATORS

Qingkun Zhou

College of Mechatronics Engineering and Automation,
National University of Defense Technology
Changsha, Hunan, P. R. China

Pinhas Ben-Tzvi

Department of Mechanical and Aerospace Engineering,
The George Washington University
Washington, DC 20052, USA

Azhar Iqbal

Department of Mechanical and Industrial Engineering,
University of Toronto
Toronto, Ont., Canada

Dapeng Fan

College of Mechatronics Engineering and Automation,
National University of Defense Technology
Changsha, Hunan, P. R. China

ABSTRACT

Magnetic micro-electro-mechanical-systems (MEMS) present new class of micro-scale devices that incorporate magnetic materials as sensing or active elements. It exploits the properties of magnetic materials by incorporating them in conventional microfabricated systems. Although their application for microactuation purposes has been limited, the prospects of remote control and large displacements renders them useful, and even unavoidable in certain circumstances. Recognizing the fact that poor electromagnetic flux in micro domain happens to be the most stringent limitation, measures to improve the magnetic field generated by an electromagnetic coil are studied using a microactuator that incorporates a coil and a hard magnetic film deposited on a flexure membrane. This paper describes the design of the microactuator, analysis and optimization that maximizes the deflection. This study also presents an overview of magnetic microactuators covering the scaling effects, materials and processes used in their fabrication and critical review of their limitations.

KEYWORDS

Magnetic MEMS, Microactuators, Electromagnetic Coils, Optimization, COMSOL

1. INTRODUCTION

Microelectromechanical systems have been playing an important role in many fields including automotive industry, communication, military, and medical applications, in order to meet compact-size and low-cost requirements. Magnetic microelectromechanical systems (MEMS) present new class of micro-scale devices that incorporate magnetic materials as sensing or active elements. The introduction of magnetic MEMS has prompted a whole new range of applications. One of the new areas of applications is microactuators. Though electrostatic microactuators have dominated the field owing to some obvious advantages like ease of integration in microelectronic systems and better force scaling, in recent years there has seen an increased interest in magnetic microactuators. The trend is driven by the unique capabilities of magnetic systems, such as wireless and bidirectional control and significantly larger actuation displacements.

Since MEMS have evolved from the microelectronics industry, electrostatic interactions have been advantaged from the very beginning as the primary actuation mechanism in these systems. A brief look into the literature reveals that earlier studies outrightly downplayed the concept of magnetic actuation [1] or drew unfavorable conclusions based on force scaling [2]. Wagner [3] and Guckel [3] were the pioneers who

designed magnetic microactuators promoting the concept. Guckel [5] remarked that permanent magnets are vital to magnetic actuation and that their integration can bring breakthrough in the application of the concept. The assertion still remains valid. A thorough analysis of the benefits of electromagnetic interactions is presented in [6]. Ahn and Allen [7] presented some valuable results in the area of RF applications and actuation using electromagnetic coils. Fang has demonstrated a reduced-order model to describe the mechanical behaviour of microbeam-based magnetic devices [8]. Jiri built a fast dynamic model of magnetic micro-actuator resulting in fast calculation of all interactions affecting a mobile magnet [9]. Zhang[10]designed a fast switching electromagnetic microactuator with two stable positions fabricated using UV-LIGA technology. Fu [11] designed a new type of electromagnetic bi-stable MEMS relay which is operated by a wiggling microactuator symmetrically assembled with two integrated planar windings and one permanent rotor in the form of sandwich with coaxial sustained gaps between each other.

This study presents an overview of the magnetic MEMS and important issues related to their incorporation in integrated or batch-fabricated microsystems. The overview includes the effects of miniaturization on the known macro-scale principles that govern the magnetic field. The scaling effects are compared with those of the other actuation mechanisms. The manufacturability of these systems is examined by reviewing the magnetic materials and processes used to integrate them in microfabrication. Keeping in view the limitations of the magnetic microactuators, the future prospects of these devices are critically reviewed.

Knowing that electromagnets scale poorly in micro-domain but are critically important for control of most of the magnetic actuators, the measures to enhance their field strength are studied using a sample actuation system comprising of an electromagnetic coil and a permanent magnet deposited on a membrane flexure. The design description and layout of the actuator is followed by modeling, analysis and optimization of the proposed design.

2. CRITICAL APPRAISAL OF MAGNETIC MEMS

2.1 Advantages of Magnetic MEMS

In addition to the high energy density available in magnetic fields, magnetic interactions offer many advantages for actuation in MEMS.

Permanent magnets provide constant magnetic fields. This means that simple or bi-stable permanent latching forces can maintain a system in a given configuration without the need for energy consumption. This feature not only ensures energy savings, but is also an excellent safety guarantee in the case of power failure in radio frequency or optical fiber communication network switchboards. Such permanent forces can also be implemented into passive magnetic

suspensions/bearings, providing an elegant solution to the problem of friction in MEMS.

Magnetic fields and gradients can be effective over long distances relative to the size of the MEMS device. This allows for large-throw and/or wide-angular actuations, for which electrostatic actuation would need unrealistic voltages.

Contactless magnetic interaction allows remote actuation through sealed interfaces. This not only enables wireless actuation but also allows vacuum packaging of resonant systems, giving them a high quality factor by avoiding dampening the vibrations due to the viscosity of the ambient air. Remote interaction also means that a macroscopic permanent magnet providing a strong static magnetic field or gradient can be appended to the system without the need to be integrated within the system, thereby simplifying fabrication. Furthermore, remote actuation through sealed interfaces makes magnetic actuators very well suited for harsh environments.

2.2 Limitations of Magnetic MEMS

According to the discussion on scaling effects, it is clear that the primary advantage of magnetic MEMS for actuation purposes lies in the use of permanent magnets. However, exploitation of their potential is limited by the following two aspects: 1) Lack of efficient fabrication and integration processes; 2) Inability to control the magnetic field without an electromagnet or externally applied field.

While the former of the two limitations is gradually being redressed by improving fabrication processes, the later remains challenging and, for applications where external application of controlling magnetic field is not feasible, electromagnetic activation and control remains the only option. This is also true for devices that need local control of actuator arrays such as micromirrors and microfluidic manipulators. As mentioned earlier, electromagnets scale poorly in micro domain and also present several problems, such as excessive heat dissipation and power consumption. Given this inevitable nature of electromagnets, the only option left is to seek their optimal performance conditions in terms of coil configurations, dimensions and current flow. Over the years, considerable research efforts have been directed to those objectives and some very innovative systems have been developed that not only defy the long-held notion of lack of usefulness of electromagnets in micro domain, but also push the frontiers of expediency of MEMS in general.

2.3 Scaling Effects

Although mechanics of micro- and nano-scale systems can be significantly different from the macroscopic laws derived on the basis of continuum mechanics approach, direct scaling of these laws does provide valuable insight into various interactions in the miniaturized domain. The relative scaling of different forces as a result of the miniaturization is the most convenient tool for analysis of the feasibility of a proposed MEMS application. The scaling effects of magnetic MEMS have been the subject of various studies, some involving

differing viewpoints. The following paragraphs present some of the leading assertions:

1) Direct Force Scaling

Trimmer [2] used a matrix formulism to describe the results of scaling of forces. Using the fundamental Maxwell equations, the forces between two current carrying conductors and those between a conductor and a permanent magnet scale as shown in Table. 1.

Tab. 1: Magnetic force scaling by Trimmer's Method

	Conductor to conductor	Conductor to permanent magnet
Constant Current Density	s^4	s^3
Constant Heat Flow/Area	s^3	$s^{2.5}$
Constant Temperature Rise across winding	s^2	s^2

2) Stored Energy Analysis

Judy and Muller [12] have been pursuing the prospect of integrating hard magnetic materials and have also presented a different perspective on the scaling issues based on energy density in different fields. It is a more elaborate approach based on total energy stored in a magnetic field and compared it with electrostatic energy for an equivalent system and thus established the cross-over point i.e., the dimensions below which the electrostatic forces dominate their magnetic counterpart. The energy density for electrostatic field is given as:

$$U_{electrostatic} = \frac{1}{2} \epsilon E^2 \quad (1)$$

where ϵ is the permittivity of the field material and E is the applied electric field. The energy density for a magnetic field is as follows:

$$U_{magnetic} = \frac{1}{2} \frac{1}{\mu} B^2 \quad (2)$$

where μ is the permeability of the field and B is the magnetic flux density. For conventional macroscopic systems the energy density of the magnetic field is of the order of 10,000 times the electrostatic field.

3) Homothetic Miniaturization of Magnetic System

The most significant application so far has been contributed by Cugat et al [13] who designed arrays of microcoils for actuation of deformable mirrors. Coining the term MAGMAS (Magnetic Micro-actuators and Systems) they have presented a very elaborate review of the scaling phenomenon of magnetic actuators. While Judy's arguments cleared some of the prevailing pessimism about magnetic MEMS, lately, Cugat et al [14] have further accentuated the effectiveness of these systems by taking a homothetic approach considering the scalar potential V of a magnetic field given as:

$$V = \frac{v}{4\pi\mu_0} \frac{\mathbf{J}\mathbf{r}}{r^3} \quad (3)$$

where v is the volume of an elementary magnet with magnetic polarization \mathbf{J} . The magnetic field \mathbf{H} at a point P is defined as the gradient of the scalar potential: $\mathbf{H} = \Delta V$.

However, the magnetic field, which is the gradient of the potential, remains unaltered. This has important implications on Laplace-Lorentz force for instance, which is proportional to the field, in a manner such that it remains unaffected. However, if the interacting element is also a ferromagnetic material, the volumetric force, which is proportional to the field gradient, is multiplied by the factor k . Conversely, the application of Biot-Savart law for the evaluation of the magnetic field between current carrying conductors results in a magnetic field that scales down by the factor k . However, when interacting with a magnet, the force applied by the conductor's field remains unaffected. The effect of scale reductions in various configurations is different.

3. MAGNETIC MATERIALS FOR MEMS

Magnetic MEMS use materials that either generate a magnetic field or help improve its strength. The magnetic materials can be classified according to their magnetic susceptibility χ and relative permeability μ_r . These properties define the constitutive relationship between the magnetic field H , the flux density B and the magnetization M . For the simplified case of the linearly magnetized materials, the relationship can be written as follows:

$$\begin{aligned} \chi &= \frac{M}{H} \\ B &= \mu_0 H + M = \mu_0 \mu_r H \end{aligned} \quad (4)$$

where μ_r is the relative permeability of vacuum. Tab.2 lists various types of magnetic materials classified according to their susceptibilities. Most of the MEMS applications with magnetic materials use the ferromagnetic materials.

Tab. 2: Magnetic Material Classification

Category	χ / μ_0	Examples
Ferromagnetic	10^7 to 10^2	Ni, Fe, Co, NiFe, NdFeB
Ferrimagnetic	10^4 to 10^1	Fe_3O_4 , ferrites, garnets
Antiferromagnetic	small	MnO, NiO, FeCO_3
Paramagnetic	10^{-3} to 10^{-6}	Al, Cr, Mn, Pt, Ta, Ti, W
Diamagnetic	-10^{-6} - -10^{-3}	Ag, Au, C, H, Cu, Si, Zn
Superconducting	-1	$\text{YbBa}_2\text{Cu}_3\text{O}_x$

Another classification of the magnetic materials is based on the properties of coercivity and saturation. Depending on these properties, the magnetic materials used for MEMS can be classified into two categories:

3.1 Soft Magnetic Materials

Characterized by small coercivity and saturation field, these materials found their way into MEMS through the recording industry. Permalloy (81% Fe, 19% Ni) is typical for these materials and has been used extensively as a magnetic core in MEMS applications. Having a high flux density, low hysteresis and near zero magnetostriction, it has been used for many years as the primary material for fabrication of magnetic heads in the recording industry. Some of the materials with magnetoresistive properties have been used in magnetometers and sensors. With externally applied strong magnetic fields, soft magnetic materials have also been used on non-magnetic flexures for actuation and sensing purposes [15]. Some of the soft magnetic materials that exhibit magnetostriction property (volume change on magnetization) have also found applications in microactuators [16].

3.2 Hard Magnetic Materials

Hard magnetic materials possess high coercivity and saturation field and thus can be used as permanent magnets. Their ability to store energy is one of the primary advantages that magnetic MEMS have over other actuation mechanisms. There are many potential candidate materials for magnet applications, and the choice of material will depend on a number of factors. Some important characteristics of high performance magnet materials are compared in Tab. 3.

Tab. 3: Characteristics of hard magnetic materials

Material	$\mu_0 M_s$ (T)	$\mu_0 H_C$ (T)	BH (kJ/m ³)	T_c (K)	Corrosion resistance
Nd ₂ Fe ₁₄ B	1.61	7.6	514	585	Poor
SmCo ₅	1.05	40	220	1000	Poor
Sm ₂ Co ₁₇	1.30	6.4	333	1173	Poor
FePt – L ₁₀	1.43	11.6	407	750	Good
CoPt – L ₁₀	1.00	4.9	200	840	Good

The energy product (BH) provides a measure for the magnet's merit, as it quantifies the amount of energy stored in the magnet. Its maximum theoretical value, which is given by $\mu_0 M_s^2/4$, may be approached for a magnet which has a high value of coercivity ($\mu_0 H_C > \mu_0 M_R$) and a value of remanence close to saturation. It should be noted that all the rare earth transition metal compounds have poor resistance to corrosion and thus must always be coated with protective layers.

Under standard application conditions, Nd-Fe-B is the most obvious choice. The high-cost of Pt may constitute an obstacle to the use of Pt-based magnets, as is the case for bulk materials. Although the material quantities involved in building sub-mm magnetic MEMS are negligible, they could easily amount to a sizeable cost when fabricated in batches. This problem is further heightened by the fact that the high density of such materials means that there is even more Pt mass involved for the same volume device.

4. FABRICATION PROCESSES

The techniques used for fabrication of magnetic MEMS are a combination of conventional integrated circuits processes together with compatible techniques for coil or magnetic film deposition. While some of the magnetic materials might need very specialized processes, most metal deposition processes like electro-deposition, sputtering and evaporation can be used for fabrication of magnetic elements in a MEMS device.

4.1 Soft Magnetic Films

In contrast to the thin film magnetic recording media, the magnetic layers in MEMS can range from sub micron to millimeter range thicknesses [17]. Therefore, the deposition processes conventionally used in the recording industry may not always be feasible for MEMS applications. For most soft magnetic films, electro-deposition is the preferred method but *chemical vapor deposition* (CVD) methods are also used.

4.2 Hard Magnetic Films

For any given magnetic material, the magnetic field generated is the function of volume and hence almost all applications utilizing hard magnetic materials require deposition of thick films. The most common and most powerful micromagnets currently used in magnetic MEMS are individually micromachined from bulk Nd-Fe-B or Sm-Co magnets generally using wire electro-discharge machining. However, this method is hardly compatible with full integration or batch fabrication [18]. Many methods have been developed to make micromagnets that provide good results, but each suffers from a moderate or major drawback. Some techniques are very well adapted to microfabrication (e.g., electroplating of Co-Pt, screen printing of bonded powders), but the resulting magnetic properties are relatively poor compared to the bulk rare-earth permanent magnets [19]. Other techniques such as pulsed laser deposition [20] or direct sintering [21], give excellent magnetic properties but either the thickness of the deposited layer is too thin or the process is too difficult to adapt to micro-technology and batch fabrication due to problems like high deposition temperature, chemical pollution, slow deposition rate and small deposition surface. An important aspect currently emerging is the patterning of thick films in order to shape the finished micromagnets [22]. Optimal magnetic orientation of micromagnets is also studied. Ideally, low temperature electroplating of fully dense rare earth-based

inter-metallic compounds or alloys would combine the full compatibility of electroplating to batch fabrication microtechnologies, with the best magnetic properties of fully dense rare-earth permanent magnets.

Overall, although an increasing number of researchers are working on it, at present there is no ideal candidate for the integration of cheap and fast fabrication of thick patterned layers of good quality permanent micromagnets that are compatible with MEMS microtechnology batch fabrication processes [22].

When magnets are deposited in film form, texture control determines not only the value of remanent magnetization achieved in the magnet itself, but also the relative orientation of magnetization with respect to the film substrate (in-plane or out-of-plane). This is very important, as it will determine the applicability of the given film magnet for a given system design. Texture control in non-epitaxial films of the materials concerned has been shown to be material dependent: $\text{Nd}_2\text{Fe}_{14}\text{B}$ can be prepared with out-of-plane texture, SmCo_5 with in-plane texture and FePt with fiber texture.

4.3 Coil Fabrication

Electromagnetic coils provide the most convenient form of control mechanisms in magnetic microactuation. Since the magnetic field generated by these coils varies with the applied current, the magnetic force between the coil and permanent magnet varies accordingly. The interaction between the two provides a means of remote control that is not afforded by any other mechanism.

There are two primary approaches to coil fabrication: standard PCB process and deposition of film. The former uses copper clad PCBs to produce coils. Currents up to $200\text{A}/\text{mm}^2$ have been reported [18]. Micromachining of films deposited using stand IC processes or advanced technologies like LIGA have the advantage of fabricating multi-layer coils. Standard IC processes are commonly used to deposit Al/Cu coils on Si substrates. Although their application is limited to a few micrometer thick films, current densities of up to $2000\text{ A}/\text{mm}^2$ can be achieved [1]. Since most of the MEMS applications require as thick as $50\mu\text{m}$ conductor films, IC processes may not always be suitable. For applications needing thick or high aspect ratio coils, processes like electroplating or LIGA are resorted to. For three-dimensional coils, approaches such as wafer bonding and through vial connections are also used. The primary role of an electromagnetic coil is to convert electrical energy into magnetic flux. To be able to concentrate the flux, coils of various shapes and configurations can be employed. Some of these configurations that can be microfabricated using photolithographic techniques are shown in Fig. 1.

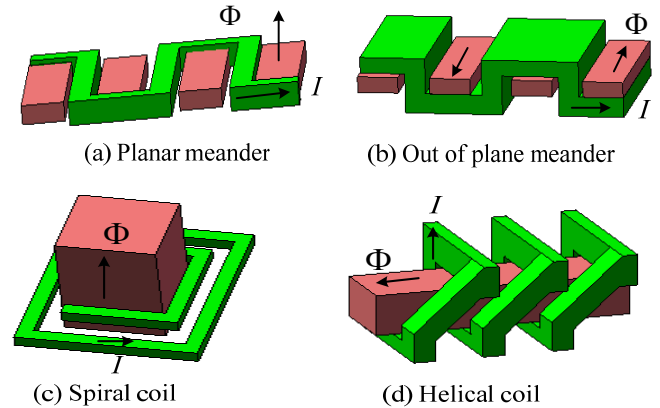


Fig. 1: Basic coil designs

5. OPTIMAL DESIGN OF ELECTROMAGNETIC COIL FOR MICROACTUATION

Recognizing the fact that electromagnets play a critically important role in the effective utilization of magnetic MEMS, the remaining part of this study will focus on the prospect of design, fabrication and optimization of a combination of an electromagnetic coil and a permanent magnet that can deliver the optimal actuation forces within the constraints of the available technologies and relatively unfavorable scaling effects. Layout and fabrication process for the actuator comprising of an electromagnetic coil and a permanent magnet deposited on a membrane flexure is described. The proposed design is modeled using COMSOL Multiphysics (FEMLAB) and the effects of the various design features of the electromagnetic coil on the actuation force are studied.

5.1 Conceptual Design of an Electromagnetic Microactuator

The principle components of an electromagnetic microactuator are a coil, a permanent magnet and a flexure membrane. Although microcoils can also be fabricated using non-lithographic methods, such as wires wound on structures and then can be assembled into MEMS devices, this study will be limited to lithographically fabricated planar coils. This is the simplest type of coils and has been used extensively in MEMS applications.

Keeping in view the properties of magnetic materials and fabrication processes discussed in Sections 03 and 4 above, an $\text{Nd}_2\text{Fe}_{14}\text{B}$ thick film will be used as the permanent magnet

The membrane is developed by microfabrication of Si substrate. The conceptual design of the proposed micro-actuator is presented in Fig. 2.

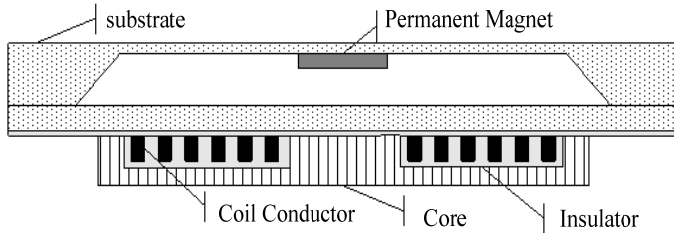


Fig. 2: Conceptual design of an electromagnetic microactuator

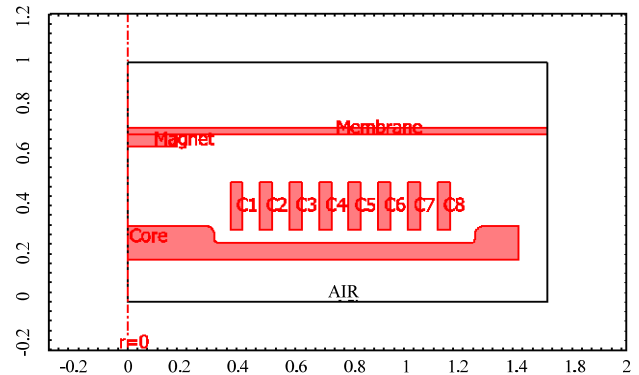


Fig. 3: COMSOL Model of Microactuator

5.2 Modeling, Simulation and Optimization of the Microactuator

The deflection of the proposed microactuator primarily depends on the magnetic force generated by the coil and the magnet, and the restoring force of the membrane. The magnetic force is determined by the magnetic field of the coil, and the strength and volume of the magnet. It is also dependent on the position of the magnet along the central axis. The restoring force of the membrane is determined by the mechanical properties of the material and the geometry of the structure. The contribution of each of the parameters is outlined in the following analysis.

1) Magnetic field of the coil

The analytical expression for the magnetic field generated by a circular coil is derived from Biot–Savart law. For a single turn coil, with radius r , the magnetic field at a distance z along its central axis is given by:

$$H(z) = \frac{Ir^2}{2(r^2 + z^2)^{3/2}} \quad (5)$$

where I is the current, r is the mean radius of the turn and z is the distance along the z -axis. To approximate the magnetic field of a coil with N turns, the contribution from each turn can be summed.

While the analytical expression can be used to make a fair estimate of the magnetic field conditions, the complex geometry warrants the use of finite element methods (FEM) for a better analysis. Therefore, the magnetic field generated by the coil was simulated using COMSOL Multiphysics FEM package. The field is modelled using a 2D axisymmetric formulation with the ‘Azimuthal Currents, Quasi-static’ application mode of the package. The mode deals with the structures that are axially symmetric around the z -axis with currents only in the angular direction. A 2D model of the actuator is shown in Fig. 3. Note that the model shows only half of the vertical cross-section. The following input parameters are used in Table 4.

Tab.4: Input parameters

	Conductivity [S/m]	Permeability [H/m]
Ni-Fe (Core)	6.71×10^6	$3000 \mu_0$
Cu (Coil)	5.95×10^7	μ_0
Air	0	μ_0

2) Magnetic force

The force applied by a magnetic field on a permanent magnet placed in the field is given as

$$F_z = B_r A_m \int_z^{z+h_m} \frac{dH}{dz} dz \quad (6)$$

where F_z is the magnetic force (considering vertical component only), B_r is the remanence of the magnetic material and, A_m and h_m are the surface area and height of the magnet, respectively. As evident from the expression, the magnetic force is proportional to the rate of change of the magnetic field with respect to z . For optimal performance, the magnet should be placed at a position where the magnetic field gradient is maximum. The force is also directly proportional to the strength and volume of the magnetic material. Therefore, to generate a large force, the magnet should have a large value of magnetic remanence and also as large a volume as possible. The magnetic force on the permanent magnet is simulated using ‘Magnetostatic, No Currents’ mode with field gradient input from the simulation of the coil as described above. The magnetic properties of Nd-Fe-B were provided as a B-H table.

3) Membrane restoring force

The linear model of the response of a membrane to a point force is:

$$F_z = -kd_z \quad (7)$$

where F_z is the force, d_z is the deflection and k is the spring constant for a particular membrane material with a given

geometry. For a given length l and thickness t equation (7) can be expanded to give the following relationship:

$$d_z = c \frac{Fl^2}{D} \quad (8)$$

where D is the flexural rigidity of the membrane material and the constant c depends on the boundary conditions at the outer edges and shape of the membrane. D is defined by:

$$D = \frac{Et^3}{12(1-\nu^2)} \quad (9)$$

where E is the Young's Modulus of the material and ν is Poisson's ratio.

The membrane is modeled in COMSOL using 'Axisymmetric Stress-strain' mode with the magnetic force determined by the solution of the magnetic field now input as edge load along the central axis. A moving mesh was used to model the coupling between the deflection and the magnetic force.

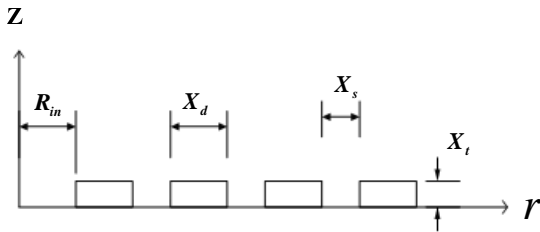


Fig. 4: Coil dimension variables

4) Simulation Results

Initial simulations are performed for a 4-turn coil of the following dimensions:

$$\begin{aligned} X_t &= 50 \mu\text{m} \\ X_d &= 200 \mu\text{m} \\ X_s &= 50 \mu\text{m} \\ R_{in} &= 300 \mu\text{m} \end{aligned} \quad (10)$$

The following *parameters* are used:

Inward current density: 100 mA

Thickness of membrane: 25 μm

Height of membrane: 400 μm above the coil base

Diameter of membrane: 3.4 mm

The electromagnetic loading on the permanent magnet element results into the following response:

Maximum deflection: 0.0829 μm

Location of Maximum deflection: $r=0$

Applied Magnetic Force: 1.68 mN

The effect of weight of membrane and the magnet was found to be negligible. Deformation of the membrane is shown in Figure 5. The magnetic field resulting from the interaction of the electromagnet and the permanent magnet is shown in Figure 6.

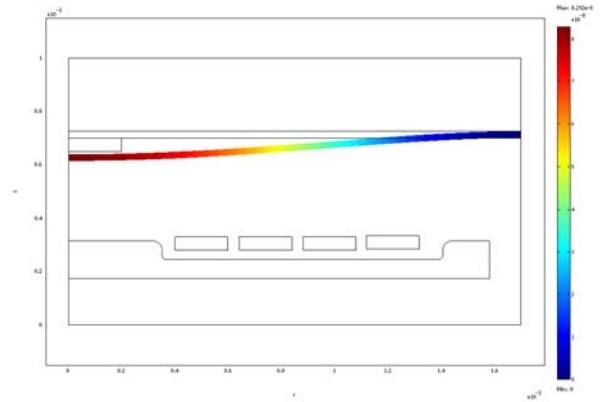


Fig. 5: Deformation of membrane

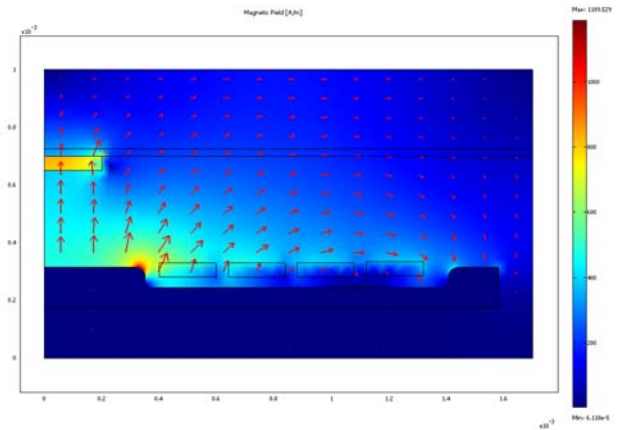


Fig.6: Surface plot of magnetic field

5.3. Design Optimization

With the aforementioned conceptual design and the FEM analysis tools, a design optimization problem can be formulated as follows:

$$\max_{x \in \Omega} d(x) \quad (11)$$

s.t.

$$\begin{aligned} 50 &\leq x_1 \leq 1000 \\ 20 &\leq x_2 \leq 300 \\ 20 &\leq x_3 \leq 300 \quad \text{units}(\mu\text{m}) \\ 20 &\leq x_4 \leq 300 \\ 350 &\leq x_5 \leq 1000 \end{aligned} \quad (12)$$

where $d(x)$ is the deflection of the membrane representing the objective function, Ω is the design space defined by limits on the vector of design variables, $x = \{x_1, x_2, x_3, x_4, x_5\}^T = \{R_{in}, X_t, X_d, X_s, h\}^T$ as defined in Fig. 4. Here the limits on the dimensions have been placed keeping in view the fabrication considerations. In order to solve the problem, the COMSOL analysis providing the deflections was fed to MATLAB

Optimization Toolbox function. Based on multiple analyses of the model, the following trends were observed:

- (1) The magnetic field strength increases almost linearly with decreasing internal radius R_m .
- (2) For constant current density and area, a high aspect ratio $X_i > X_d$ coil results in higher field strength.
- (3) For a given footprint, decreasing the separation X_s between coils increases the field strength.
- (4) Increasing the number of turns increases the field; however, the effect diminishes quickly with increasing numbers.
- (5) The gradient $\left(\frac{\partial H}{\partial z}\right)$ is always negative implying

increasing force with decreasing separation at any particular radial location. For a given height h above the coil base, the radial location of points of maximum field strength and its gradient vary considerably (Fig. 7). The optimal point is determined by the optimization algorithm. The surface plot of the magnetic field obtained for the turn coil case is given in Fig. 8.

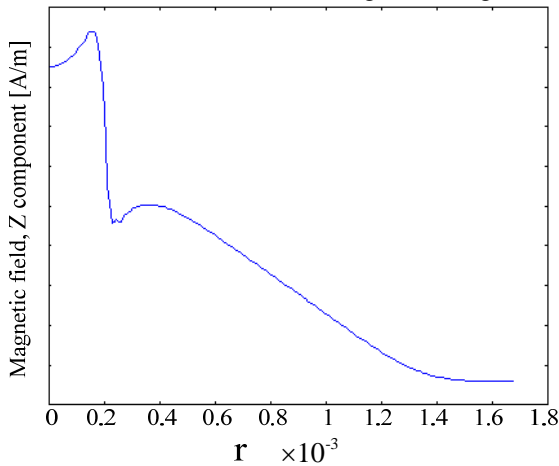


Fig. 7: Radial variation of the magnetic field ($z=275 \mu\text{m}$)

Considering these trends and having solved multiple optimization problems with varying number of turns, the following best design conditions were obtained:

Maximum deflection: $0.91 \mu\text{m}$

Maximum force: 21.85 mN

$$\begin{aligned} R_m &= 50 \mu\text{m} \\ X_i &= 40 \mu\text{m} \\ X_d &= 250 \mu\text{m} \\ X_s &= 20 \mu\text{m} \\ h &= 350 \mu\text{m} \end{aligned} \quad (13)$$

No. of turns = 8

Thickness of membrane = $15 \mu\text{m}$

where the dimensions have been rounded to the nearest tens of micrometers.

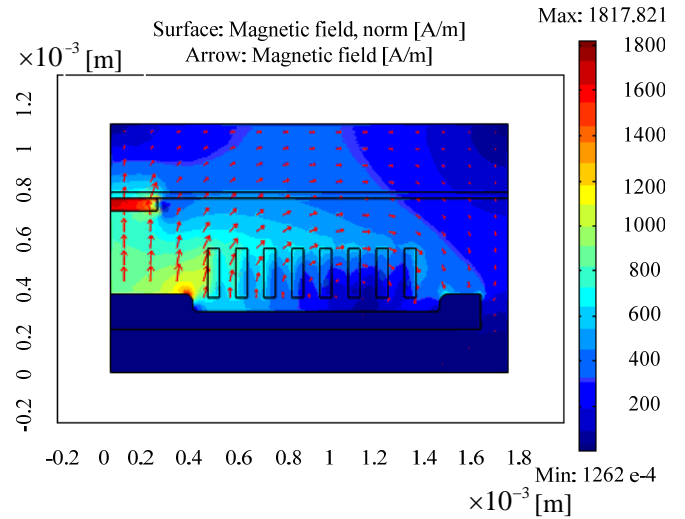


Fig. 8: Surface plot of the magnetic field

5.4. Microfabrication Recipe

The coil is fabricated by electroplating Cu layer on Si substrate and a soft magnetic Ni-Fe layer that serves as the core. The membrane is formed by bulk micromachining of another Si substrate. The magnet is fabricated by sputtering $\text{Nd}_2\text{Fe}_{14}\text{B}$ on to the inner surface of the membrane.

The five mask fabrication process is shown in Fig. 8 and the important steps of the process are described below:

Step (a)

- (1) Pattern the spiral planar coil on silicon wafer having preprocessed insulation film.
- (2) Electroplate the copper layer.
- (3) Recover the coil structure by removing the first mask.

Step (b)

- (1) Pattern for insulator.
- (2) Sputter the SiO_2 layer.
- (3) Remove second mask to recover the insulator layer.

Step (c)

- (1) Pattern the magnetic core.
- (2) Electroplate the Ni-Fe layer.
- (3) Remove third mask to recover the core.

Step (d)

- (1) Dope the other Si substrate to etch stopping thickness.

Step (e)

- (1) Pattern the other face of the second substrate for membrane.
- (2) Bulk micro machine using KOH to form membrane.
- (3) Remove pattern.

Step (f)

- (1) Pattern for the electromagnet on the inner surface of the membrane.

- (2) Sputter the $\text{Nd}_2\text{Fe}_{14}\text{B}$ layer.

- (3) Remove pattern to recover the magnet.

Step (g)

(1) Fusion bond the two wafers to assemble the device.

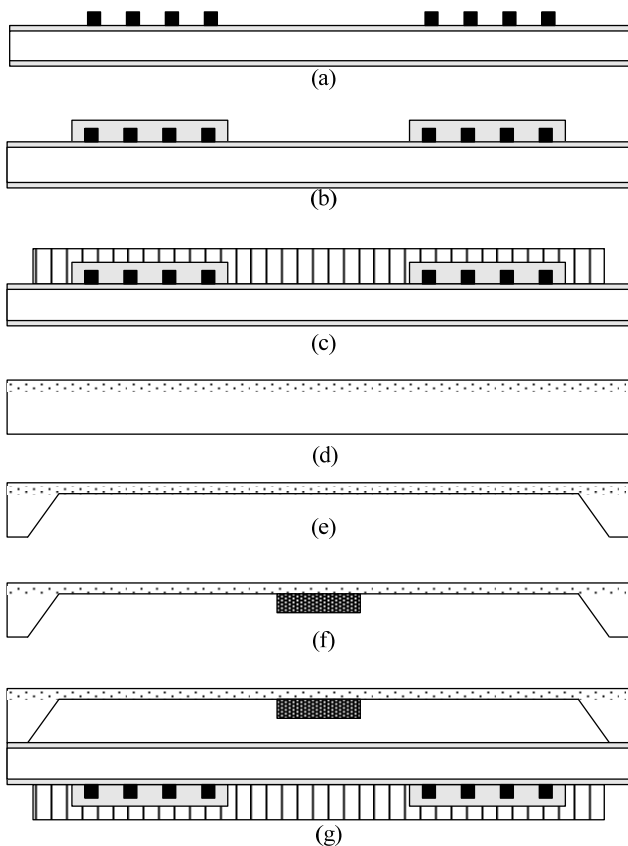


Fig. 7: Fabrication Layout

6. CONCLUSION

Although difficulties in fabrication and some of the pessimistic views in past have limited the wide spread applications of magnetic actuators, the growing awareness of their usefulness foretells a future not as bleak as initially viewed. With improving fabrication processes for hard magnetic materials, magnetic microactuation will remain as pertinent as in macroscopic domain. Especially for applications needing arrays of actuators with large deflections, the combination of electromagnets and hard magnetic materials seems to be the most viable solution.

REFERENCES

- [1] Feynman, R.P., 1992, "There's plenty of room at the bottom", *Journal of Microelectromechanical Systems*, **1**, pp. 60-66.
- [2] Trimmer, W.S.N., 1989, "Microrobots and micromechanical systems", *Sensors and Actuators*, **19**, pp. 267-287.
- [3] Wagner, B., Benecke, W., 1990, "Magnetically driven micro-actuators: Design considerations", *Microsystems Technologies*, pp. 838-843.
- [4] Guckel, H., 1991, "Fabrication and testing of the planar magnetic micromotor", *Journal of Micromechanics and Microengineering*, **1**, pp. 135-138.
- [5] Guckel, H., 1996, "Progress in electromagnetic actuators", *Proceedings Actuator' 96, Bremen, Germany*, pp. 45-48.
- [6] Busch-Vishniac, I.J., 1992, "The case for magnetically driven microactuators", *Sensors and Actuators A: Physical*, **33**, pp. 207-220.
- [7] Ahn, C. H., Allen, M. G., 1998, "Micromachined planar inductors on silicon wafers for MEMS applications", *IEEE Transactions on Industrial Electronics*, **45**, pp. 866-876.
- [8] Fang, Y. M., Huang, Q.A., Li W.H., "A dynamic macromodel for distributed parameter magnetic microactuators", *Chinese Physics B*, **17(5)**, 2008, pp: 1709-1715.
- [9] Štěpánek, J., Rostaing, H., Delamare, J., Cugat, O., 2004, "Fast dynamic modeling of magnetic micro-actuator", *Journal of Magnetism and Magnetic Materials*, **272(1)**, pp.669-671
- [10] Zhang, Y.-H., Ding, G. F., Dai, X.H., Cai, B. C., 2005, "Fast switching bistable electromagnetic microactuator", *Electronics Letters*, **41(23)**, pp.1276-1278.
- [11] Fu, S., 2007, "Design and fabrication of a magnetic bistable electromagnetic MEMS relay", *Microelectronics Journal*, **38**, pp. 556-563.
- [12] Judy, J.W. and Muller, R. S. 1997, "Magnetically actuated, addressable microstructures", *Journal of Microelectromechanical Systems*, **6**, pp. 249-256.
- [13] Cugat, O., Basrour, S., Divoux, C., Mounaix, P., Reyne, G., 2001, "Deformable magnetic mirror for adaptive optics: technological aspects", *Sensors and Actuators A: Physical*, **89**, pp. 1-9.
- [14] Cugat, O., Delamar, J., Reyne, G., 2003, "Magnetic micro-actuators and systems (MAGMAS)", *IEEE Transactions on Magnetics*, **39**, pp. 3607-3612.
- [15] Niarchos, D., 2003, "Magnetic MEMS: key issues and some applications", *Sensors and Actuators A: Physical*, **109**, pp. 166-173.
- [16] Bhailís, D. de., Murray, C., Duffy, M., Alderman, J., Kelly, G., and Mathúna, S.C. Ó., 2000, "Modelling and analysis of a magnetic microactuator," *Sensors and Actuators A: Physical*, **81**, pp. 285-289.

[17] Kohlmeier, T., Seidemann, V., Büttgenbach, S., Gatzen, H.H., 2004, “An investigation on technologies to fabricate microcoils for miniaturized actuator systems”, *Microsystem Technologies*, **10**, pp. 175-181.

[18] Jang, Y.H., Kim, Y. K., 2003, “Design, fabrication and characterization of an electromagnetically actuated addressable out-of-plane micromirror array for vertical optical source applications” , *Journal of Micromech Microengineering*, **13**, pp. 853-863.

[19] Cho, H. J. and Ahn, C. H., 2000, “Electroplated Co-Ni-Mn-P-based hard magnetic arrays and their applications to microactuators” , in *Proc. Electro-Chemical Soc.*, pp. 586.

[20] Cadieu, F. J., Rani, R., Qian, X. R., and Chen, L., 1998, “High coercivity Sm-Co based films made by pulsed laser deposition,” *Journal of Appl. Phys.*, **83(11)**, pp. 6247–6249.

[21] Yamashita, F., 2002, “Preparation of thick-film Nd-Fe-B magnets by direct Joule heating”, *Proc. REM XVII*, Newark, DE, pp. 668–674.

[22] Budde T., Gatzen, H. H., 2002, “Patterned sputter deposited Sm-Co films for MEMS applications”, *Journal of Magnetism and Magnetic Materials*, pp.1146-1148.